

Antisite traps and metastable defects in Cu(In,Ga)Se₂ thin-film solar cells studied by screened-exchange hybrid density functional theory

Johan Pohl,¹ Thomas Unold,² and Karsten Albe¹

¹*Institut für Materialwissenschaft, Technische Universität Darmstadt, Petersenstr. 32, D-64287 Darmstadt, Germany*

²*Helmholtz-Zentrum Berlin, Hahn-Meitner-Platz 1, D-14109 Berlin, Germany*

(Dated: March 3, 2013)

Electronic structure calculations within screened-exchange hybrid density functional theory show that Cu_{In,Ga}⁰ antisites in both CuInSe₂ and CuGaSe₂ are localized hole traps, which can be attributed to the experimentally observed N2 level. In contrast, Ga_{Cu} antisites and their defect complexes with copper vacancies exhibit an electron trap level, which can limit the open-circuit voltage and efficiency in Ga-rich Cu(In,Ga)Se₂ alloys. Low-temperature photoluminescence measurements in CuGaSe₂ thin-film solar cells show a free-to-bound transition at an energy of 1.48 eV, in very good agreement with the calculated transition energy for the Ga_{Cu} antisite. Since the intrinsic DX center In_{DX} does not exhibit a pinning level within the band gap of CuInSe₂, metastable DX behaviour can only be expected for Ga_{Cu} antisites.

Thin-film solar cells with absorbers based on Cu(In,Ga)Se₂ alloys currently achieve record efficiencies of 20.3% and represent one of the most promising technology for large-scale industrial production [1]. Efficiencies up to 14.2% can also be obtained with the ternary boundary phase CuInSe₂, whereas the efficiencies of pure CuGaSe₂ cells are still limited to below 10 % [2]. Intrinsic point defects acting as recombination centers are likely to limit the open-circuit voltage and therefore the solar cell efficiency of these absorbers. The point defect physics of these chalcopyrites has been extensively studied by experimental methods, such as electrical and optical spectroscopy methods, and theoretical approaches, mostly calculations based on density functional theory [3–13]. A hole trap level in the range between 0.15–0.35 eV, often named N2, has been observed using admittance and deep-level transient spectroscopy (DLTS) and Hall measurements in CuInSe₂ [14–16], CuGaSe₂ [15–19] and Cu(In,Ga)Se₂ [14, 15, 20–22]). A measured activation energy between 0.05–0.20 eV, has been attributed to an interface defect in Cu(In,Ga)Se₂ and was named N1 [20], although this denomination is ambiguously used and it is unclear whether the N1 response is associated to a defect at all [23]. Indeed, various metastable effects have been observed in CIGSe devices such as persistent photoconductivity [24], the increase of the open-circuit voltage upon white-light soaking [25], an increase of the space-charge upon illumination [26] or reverse-biasing [27] accompanied with a decrease of the fill factor [28] as well as capacitance relaxation on long time scales after light-soaking [29].

Based on electronic structure calculations within local density functional theory, two intrinsic point defects and their complexes with copper vacancies have been proposed to exhibit metastable properties in CuInSe₂ and CuGaSe₂: the intrinsic indium and gallium DX centers (In, Ga)_{DX} [10][30] and the selenium vacancy V_{Se} [8] or selenium vacancy–copper vacancy complex V_{Se} – V_{Cu} [9].

These theoretical results have been invoked [31–34] to explain the experimentally observed light and voltage-bias induced metastabilities. However, metastable point defects are not the only possible explanation. Copper migration in the space charge region [35, 36], deep acceptor levels in the CdS buffer layer [37], an electron-injection dependent barrier at the molybdenum back-contact of the device [23], or the presence of a p+-layer in conjunction with a shallow donor level at the buffer absorber interface [38] have all been put forward as possible explanations. Therefore, metastabilities in Cu(In,Ga)Se₂ based devices and their possible relation to the N2 and N1 levels remain puzzling and it is not clear whether a single explanation is sufficient to explain all of the observed phenomena [23, 39]. Despite extensive efforts, no concise picture of the point defect physics that matches with all of the experimental findings has yet emerged.

In this letter, we show that Cu_{In,Ga}⁰ antisites are localized hole traps in both CuInSe₂ and CuGaSe₂, which can be attributed to the experimentally observed N2 level, while Ga_{Cu} antisites and their defect complexes with copper vacancies exhibit an electron trap level, which can limit the open-circuit voltage and efficiency in Ga-rich Cu(In,Ga)Se₂ alloys. Our results are based on electronic structure calculations within screened-exchange hybrid density functional theory and are put in context to low-temperature photoluminescence measurements of CuGaSe₂ thin-film solar cells.

We have carried out hybrid density functional calculations using the HSE06 functional [40, 41] as implemented in VASP [42] with an adapted exchange-screening parameter of 0.13 Å⁻¹ [43], which allows to closely match the experimentally observed band gaps for both CuInSe₂, CuGaSe₂ and other chalcopyrite phases [11]. The approach allows to overcome the band-gap problem, to directly analyze defect levels within the gap and improves the description of localized and correlated copper *d* electrons [44, 45]. Thus, using the HSE06 functional will lead to more accurate formation enthalpies of point de-

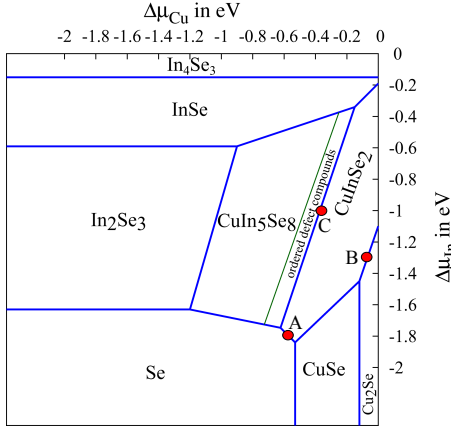


FIG. 1. Stability diagram for CuInSe₂. The defect formation enthalpies in Fig. 2 are discussed in terms of the chemical potential at points A, B and C. The stability range for CuGaSe₂ (not shown) has the same shape, but a somewhat larger extent due to its higher formation enthalpy (CuInSe₂: -2.37 eV, CuGaSe₂: -2.67 eV).

fects than LDA calculations. A 2x2x2 Γ -centered k-point grid has been used for supercells with 64 atoms as well as with 216 atoms. Ion positions were relaxed until forces were converged to below 0.05 and 0.1 eV/Å, for supercells of 64 and 216 atoms, respectively. The calculation of supercells of 216 atoms with a 2x2x2 k-point grid are computationally extremely costly, but necessary in order to observe unambiguously localized defect levels of $\text{Cu}_{\text{In,Ga}}^0$ and Ga_{Cu}^0 . All reference phases presented in the stability diagram (Fig. 1) were calculated using the same functional. The point defect formation enthalpies were calculated as function of the chemical potentials of the constituents $\Delta\mu_i$ referenced to the elemental phases and the Fermi energy ϵ_F according to the common formula as e.g. in Ref. [7]. The potential alignment and image charge corrections have been carefully carried out as described in Ref. 46.

Since high-efficiency Cu(In,Ga)Se₂ absorber material is prepared under a highly selenium-rich atmosphere, e.g. with a selenium to metal flux ratio of 5 [47], it is instructive to interpret the defect physics for this material under selenium-rich conditions on the Se-Cu(In,Ga)Se₂ phase boundary in the calculated stability diagram (point A in Fig. 1). In contrast to a previously calculated stability diagram [7], our calculations show a phase boundary between Cu₂Se and CuInSe₂, which is in line with the experimental phase diagram and the observation of Cu₂Se precipitates under certain processing conditions[48] (point B). For Cu-poor compositions, which yield the highest conversion efficiency, Cu(In,Ga)Se₂ is a highly compensated semiconductor. In this case, the charge neutrality condition and thus the Fermi-energy is essentially determined by the concentration of donors and acceptors with the lowest formation

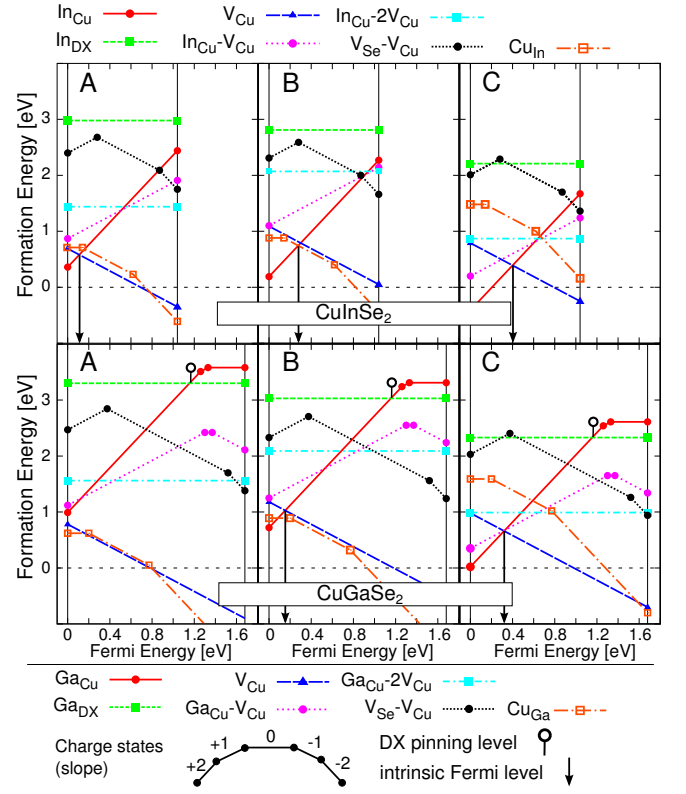


FIG. 2. Defect formation enthalpies, charge transition levels and the determined intrinsic Fermi levels in CuInSe₂ and CuGaSe₂ for chemical potentials corresponding to points A, B and C in Fig. 1.

energies (see Fig. 2). For the chemical potentials at points A, B and C the material turns out to be p-type, while it becomes n-type for maximal Cu- and In-rich conditions (not shown). Fig. 2 shows the calculated defect formation enthalpies for the various chemical potentials.

One of the most intriguing result is that $\text{Cu}_{\text{In,Ga}}$ antisites in both materials, CuInSe₂ and CuGaSe₂, can have equally low formation enthalpies as copper vacancies and thus also act as compensating defects. This finding is consistent with large concentrations of Cu_{In} in CuInSe₂ recently reported using wavelength dispersive x-ray diffraction even for copper-poor material [49]. However, when the chemical potentials are shifted towards metal-rich conditions (e.g. point C), it is seen that the formation enthalpy of $\text{Cu}_{\text{In,Ga}}$ at the intrinsic Fermi level (vertical arrow) increases, while it does not change much for $(\text{In,Ga})_{\text{Cu}}$ and V_{Cu} .

The analysis of the density of states of $\text{Cu}_{\text{In,Ga}}^0$ and $\text{In}_{\text{Cu,Ga}}^0$ reveals an empty narrow defect band above the VBM for Cu_{In} in CuInSe₂ (at 0.27 eV) and Cu_{Ga} in CuGaSe₂ (at 0.32 eV), which can trap two holes (the hole density of the empty single-particle defect state of Cu_{Ga} as obtained from the calculation is displayed in Fig. 4). Furthermore, a localized electron trap level emerges for Ga_{Cu}^0 at a single-particle energy of 1.17 eV above the

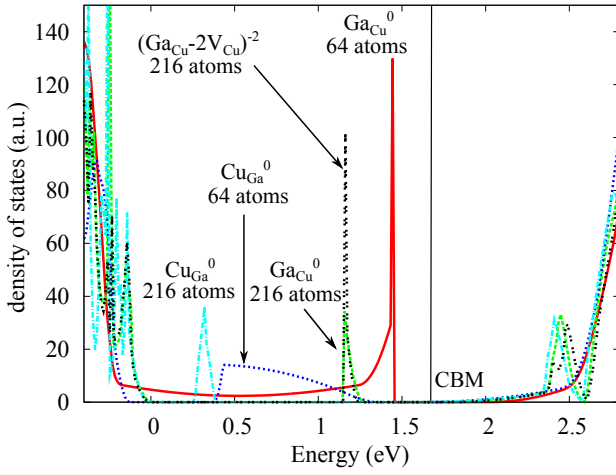


FIG. 3. Aligned density of states of CuGa^0 , GaCu^0 and $(\text{GaCu} - 2\text{V}_{\text{Cu}})^{-2}$ in CuGaSe_2 in supercells of 64 and 216 atoms as obtained with the adapted HSE06 functional.

VBM in CuGaSe_2 (see also Fig. 4). Forming defect complexes such as $\text{GaCu} - \text{V}_{\text{Cu}}^-$ and $(\text{GaCu} - 2\text{V}_{\text{Cu}})^{-2}$, does not affect the position of the defect level. The defect level of In_{Cu}^0 is found to be resonant within the CB for CuInSe_2 at 1.48 eV and for CuGaSe_2 at 1.46 eV approximately independent of gallium content. All individual single-particle defect levels are approximately constant on an absolute energy scale, when comparing their position in CuInSe_2 and CuGaSe_2 relative to the respective VBM. However, the defect levels of In_{Cu}^0 and GaCu^0 as individual defects do not align on an absolute scale, the In_{Cu}^0 defect level being 0.29-0.41 eV higher than the one of GaCu^0 in both CuInSe_2 and CuGaSe_2 as host material.

Here it should be noted that defect calculations on $\text{Cu}(\text{In,Ga})\text{Se}_2$ have so far been performed with supercells smaller or equal to 64 atoms. However, very disperse defect bands appear within the gap for the cells with 64 atoms (see Fig. 3), which indicates significant self-overlap of the defect wavefunctions. If local or semilocal density functionals are used, delocalization also occurs in large supercells up to 216 atom, which is why localized deep hole traps have not been identified in the past. This proves that an accurate nonlocal treatment of exchange and correlation and large supercells are crucial for obtaining the correct localization behaviour of the $\text{Cu}_{\text{In,Ga}}^0$ defect.

The $\text{Cu}_{\text{In,Ga}}$ antisites localize holes, are abundant under typical preparation conditions (up to 10^{20}cm^{-3} at 850 K deposition temperature and the calculated thermal transition energy for the process $\text{Cu}_{\text{Ga}}^- + h_{\text{VB}}^+ \rightarrow \text{Cu}_{\text{Ga}}^0$ of 0.20 eV agrees with experimental measurements (e.g. 0.1-0.3 eV in Ref. [22] and 0.1-0.2 eV in Ref. [21]). Given these evidences it is safe to conclude that the N2 hole trap level is due to the $\text{Cu}_{\text{In,Ga}}$ antisite. The fact that this level does not occur in all samples can be explained

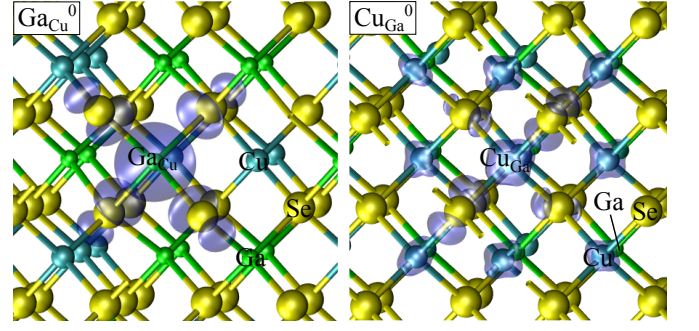


FIG. 4. Defect level electron charge density of GaCu^0 (left: isosurface $0.03 \text{ e}\text{\AA}^{-3}$) and hole density of CuGa^0 (right: isosurface $0.02 \text{ e}\text{\AA}^{-3}$) as obtained in supercells with 216 atoms.

with differing formation enthalpies relevant for different preparation conditions (compare points A,B,C in Fig. 2).

The GaCu^0 antisite, in contrast, shows a clearly localized electron trap level at a single-particle energy of 1.17 eV above the VB in CuGaSe_2 and at 1.07 eV in CuInSe_2 very close to the CBM. Therefore this antisite defect becomes increasingly deep when Ga is alloyed into CuInSe_2 , due to the rising CB. Since GaCu^0 is expected to occur in large quantities in $\text{Cu}(\text{In,Ga})\text{Se}_2$ due to its low formation enthalpy, it may limit solar cell efficiency when Ga alloying is used to increase the band-gap: When the CBM is raised above the position of the GaCu defect level, recombination through this defect may limit the open-circuit voltage. Since the associates of GaCu with copper vacancies display the same single-particle defect level as the non-complexed antisite, the complexes may cause the same limitations. With regard to the defect complexes $(\text{In,Ga})_{\text{Cu}} - 2\text{V}_{\text{Cu}}^0$ we find that their formation enthalpies are not particularly low (Fig. 2). In fact, the total binding energy of the complexes with respect to the isolated charged species is only about 0.3 eV.

It might be tempting to relate the experimentally observed N1 signature to the normal configuration of the GaCu defect in $\text{Cu}(\text{In,Ga})\text{Se}_2$. However, we note that such an assignment is contradicted by the observation of N1 in pure CuInSe_2 and the fact that its activation energy does not change with increasing Ga-content [51, 52].

To confirm our theoretical results for the GaCu defect, we conducted temperature-dependent photoluminescence measurements on a CuGaSe_2 thin-film solar cells prepared by a three-stage coevaporation process, as used for high-efficiency chalcopyrite solar cell devices[2]. For the thin film absorber investigated, a ratio $[\text{Cu}]/[\text{Ga}] = 0.87$ was measured by x-ray fluorescence analysis and the accompanying solar cell showed a device efficiency of 7%. Photoluminescence (PL) was measured using a 670 nm diode-laser as excitation source and a thermoelectrically-cooled InGaAs array coupled to a 0.5 m spectrograph for luminescence detection, with the sample placed in a closed-cycle helium cryostat. A pho-

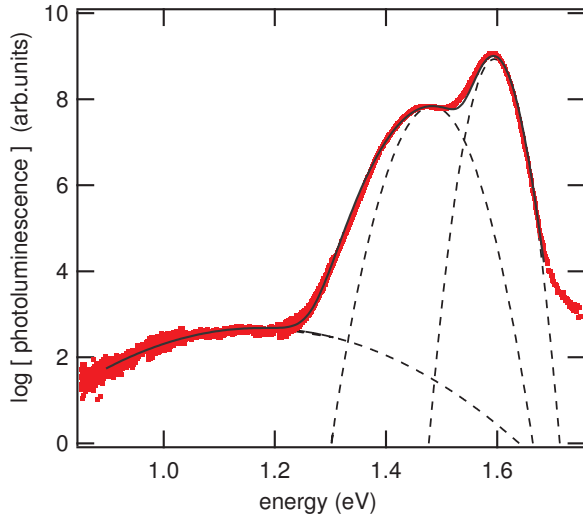


FIG. 5. Photoluminescence spectrum at $T=15$ K measured for CuGaSe₂ thin films. The black solid line indicates a fit consisting of three gaussian-shaped transitions at $E_1 = 1.6$ eV, $E_2 = 1.48$ eV and $E_3 = 1.17$ eV (dashed lines).

toluminescence spectrum obtained at 15 K is shown in Fig. 5. Three recombination peaks located at 1.6 eV, 1.48 eV and 1.17 eV can be clearly distinguished. The temperature and excitation intensity dependence of these peaks is consistent with an assignment of the peak at 1.6 eV to a tail-to-band transition, commonly observed in Cu-poor chalcopyrites [53], and the assignment of the peak at 1.48 eV to a free-to-bound transition. The latter transition energy is in excellent agreement with the calculated optical emission energy for the recombination process $\text{Ga}_{\text{Cu}}^+ + h_{\text{VB}}^+ \rightarrow \text{Ga}_{\text{Cu}}^{++}$ in CuGaSe₂ (1.44 eV) [54]. The temperature and excitation dependence of the third broad peak observed at about 1.17 eV is consistent with a donor-acceptor transition. A possible candidate for this transition is the process $\text{Ga}_{\text{Cu}}^+ + \text{Cu}_{\text{Ga}}^0 \rightarrow \text{Ga}_{\text{Cu}}^{++} + \text{Cu}_{\text{Ga}}^{-1}$, i.e. the recombination of a single electron localized on a Ga_{Cu} antisite with a neighbouring Cu_{Ga} hole trap by radiative tunneling, which has a calculated transition energy of 1.02 eV.

For metastabilities originating from intrinsic DX centers to occur, it is necessary that a DX pinning level exists within the gap[10]. From our results (Fig. 2), we conclude that such a pinning level only occurs for Ga_{Cu} antisites in CuGaSe₂ ($E_{\text{DX, pin}}^{\text{CuGaSe}_2} = 1.16$ eV), but not for In_{Cu} antisites in CuInSe₂ ($E_{\text{DX, pin}}^{\text{CuInSe}_2} = 1.31$ eV, well above the CB). Therefore, Fermi-level pinning and metastable effects due to intrinsic DX centers may occur in larger band gap Cu(In,Ga)Se₂ materials, but not for the ternary CuInSe₂. In order to assess the energy differences responsible for the different DX pinning levels as compared to Ref. [10], it is instructive to compare the *uncorrected* formation enthalpies of $\text{In}_{\text{Cu}}^{2+}$ and In_{DX} in

CuInSe₂ within our approach to the ones obtained from LDA applying only the static +U valence band correction of Ref. [10], which we were able to reproduce. The uncorrected formation enthalpy of $\text{In}_{\text{Cu}}^{2+}$ within our approach is 0.4 eV lower, while the one of In_{DX} is 0.32 eV higher. These energy differences, which result from the different treatments of exchange and correlation within HSE06 as compared to the LDA, which result mostly from the improved description of the Cu *d* electrons, directly cause the change in the DX pinning levels.

We have also investigated $V_{\text{Se}} - V_{\text{Cu}}$ vacancy pairs, which have been held responsible for a variety of metastability phenomena in Cu(In,Ga)Se₂. With respect to this defect pair our hybrid functional calculations yield comparable charge transition levels (+/-) and metastable relaxation behavior as previously found in LDA-based calculations [9]. However, the formation enthalpies of this defect complex are higher than 2 eV at the relevant Fermi levels at points A,B and C in Fig. 2). Thus, under thermal equilibrium conditions, $V_{\text{Se}} - V_{\text{Cu}}$ associates should occur only in minor quantities (below 10^{12}cm^{-3} at 850 K deposition temperature as estimated from the formation enthalpies). Thus, these defects can only cause metastable phenomena if the material is prepared under far-from-equilibrium conditions.

In conclusion, we have shown that Cu_{In,Ga} defects create a localized hole trap level in both CuInSe₂ and CuGaSe₂. Given the large amount of experimental evidence for a hole trap level in the range 0.15-0.35 eV, we conclude that Cu_{In,Ga} defects should be assigned to the N2 level. Ga_{Cu}⁰ and its complexes display a localized defect level within the gap in CuGaSe₂ and CuInSe₂. These defects are thus a likely cause for the limited efficiency of CuGaSe₂ based wide band devices. Since In_{DX}^0 does not exhibit a Fermi pinning level in CuInSe₂, metastable DX behaviour can only be expected for Ga_{Cu} antisites.

We acknowledge useful discussions with Dr. Péter Ágoston and Prof. Andreas Klein (TUD), Dr. R. Caballero for CuGaSe₂ sample growth, S. Kretschmar for the photoluminescence measurements, grants of computer time on JUROPA at the Jülich Supercomputing Center and funding within the GRACIS project (BMBF).

-
- [1] P. Jackson, D. Hariskos, E. Lotter, S. Paetel, R. Wuerz, R. Menner, W. Wischmann, and M. Powalla, Prog. Photovoltaics **19**, 894 (2011).
 - [2] R. Caballero, C. A. Kaufmann, M. Cwil, C. Kelch, D. Schweigert, T. Unold, M. Rusu, H. W. Schock, and S. Siebentritt, J. Phys. Cond. Matter **19**, 356222 (2007).
 - [3] S. Zhang, S. Wei, and A. Zunger, Phys. Rev. Lett. **78**, 4059 (1997).
 - [4] S. Zhang, S.-H. Wei, A. Zunger, and H. Katayama-Yoshida, Phys. Rev. B **57**, 9642 (1998).
 - [5] S.-H. Wei, S. Zhang, and A. Zunger, Appl. Phys. Lett.

- 72**, 3199 (1998).
- [6] Y. Zhao, C. Persson, S. Lany, and A. Zunger, *Appl. Phys. Lett.* **85**, 5860 (2004).
 - [7] C. Persson, Y.-J. Zhao, S. Lany, and A. Zunger, *Phys. Rev. B* **72**, 035211 (2005).
 - [8] S. Lany and A. Zunger, *Phys. Rev. B* **72**, 035215 (2005).
 - [9] S. Lany and A. Zunger, *J. Appl. Phys.* **100**, 113725 (2006).
 - [10] S. Lany and A. Zunger, *Phys. Rev. Lett.* **100**, 016401 (2008).
 - [11] J. Pohl and K. Albe, *J. Appl. Phys.* **108**, 023509 (2010).
 - [12] J. Pohl, A. Klein, and K. Albe, *Phys. Rev. B* **84**, 121201 (2011).
 - [13] L. E. Oikonen, M. G. Ganchenkova, A. P. Seitsonen, and R. M. Nieminen, *J. Phys. Cond. Matter* **23**, 422202 (2011).
 - [14] T. Walter, R. Herberholz, C. Muller, and H. W. Schock, *Journal of Applied Physics* **80**, 4411 (1996).
 - [15] G. Hanna, A. Jasenek, U. Rau, and H. W. Schock, *Phys. Status Solidi A* **179**, R7 (2000).
 - [16] V. Mertens, J. Parisi, and R. Reineke-Koch, *J. Appl. Phys.* **101**, 104507 (2007).
 - [17] A. Jasenek, U. Rau, V. Nadenau, and H. W. Schock, *J. Appl. Phys.* **87**, 594 (2000).
 - [18] S. Siebentritt and T. Rissom, *Appl. Phys. Lett.* **92**, 062107 (2008).
 - [19] A. Krysztopa, M. Igalson, P. Zabierowski, J. Larsen, Y. Aida, S. Siebentritt, and L. Guetay, *Thin Solid Films* **519**, 7308 (2011).
 - [20] R. Herberholz, M. Igalson, and H. W. Schock, *J. Appl. Phys.* **83**, 318 (1998).
 - [21] D. J. Schroeder, J. L. Hernandez, G. D. Berry, and A. A. Rockett, *J. Appl. Phys.* **83**, 1519 (1998).
 - [22] J. T. Heath, J. D. Cohen, and W. N. Shafarman, *J. Appl. Phys.* **95**, 1000 (2004).
 - [23] T. Eisenbarth, R. Caballero, M. Nichterwitz, C. Kaufmann, H. Schock, and T. Unold, *J. Appl. Phys.* **110**, 094506 (2011).
 - [24] T. Meyer, F. Engelhardt, J. Parisi, and U. Rau, *Journal of Applied Physics* **91**, 5093 (2002).
 - [25] M. Ruberto and A. Rothwarf, *J. Appl. Phys.* **61**, 4662 (1987).
 - [26] M. Igalson and H. W. Schock, *J. Appl. Phys.* **80**, 5765 (1996).
 - [27] R. Herberholz, U. Rau, H. Schock, T. Haalboom, T. Godecke, F. Ernst, C. Beilharz, K. Benz, and D. Cahen, *Eur. Phys. J.: Appl. Phys.* **6**, 131 (1999).
 - [28] M. Igalson, M. Bodegard, L. Stolt, and A. Jasenek, *Thin Solid Films* **431**, 153 (2003).
 - [29] F. Engelhardt, M. Schmidt, T. Meyer, O. Seifert, J. Parisi, and U. Rau, *Physics Letters A* **245**, 489 (1998).
 - [30] Intrinsic DX centers in CIGS can be regarded as (In,Ga)_{Cu} antisites displaced to a three-fold coordinated off-lattice site, which may then act as recombination centers because they exhibit defect levels within the gap [10].
 - [31] M. Cwil, M. Igalson, P. Zabierowski, and S. Siebentritt, *J. Appl. Phys.* **103**, 06370119 (2008).
 - [32] A. Urbaniak and M. Igalson, *J. Appl. Phys.* **106**, 063720 (2009).
 - [33] M. Igalson, A. Urbaniak, and M. Edoff, *Thin Solid Films* **517**, 2153 (2009).
 - [34] S. Siebentritt, M. Igalson, C. Persson, and S. Lany, *Prog. Photovoltaics* **18**, 390 (2010).
 - [35] M. Burgelman, F. Engelhardt, J. F. Guillemoles, R. Herberholz, M. Igalson, R. Klenk, M. Lampert, T. Meyer, V. Nadenau, A. Niemegeers, et al., *Prog. Photovoltaics* **5**, 121 (1997).
 - [36] J.-F. Guillemoles, L. Kronik, D. Cahen, U. Rau, A. Jasenek, and H.-W. Schock, *J. Phys. Chem. B* **104**, 4849 (2000).
 - [37] I. Eisgruber, J. Granata, J. Sites, J. Hou, and J. Kessler, *Solar Energy Materials and Solar Cells* **53**, 367 (1998).
 - [38] A. Niemegeers, M. Burgelman, R. Herberholz, U. Rau, D. Hariskos, and H. W. Schock, *Progress In Photovoltaics* **6**, 407 (1998).
 - [39] S. Siebentritt, *Solar Energy Materials and Solar Cells* **95**, 1471 (2011).
 - [40] J. Heyd, G. Scuseria, and M. Ernzerhof, *J. Chem. Phys.* **118**, 8207 (2003).
 - [41] J. Heyd, G. Scuseria, and M. Ernzerhof, *J. Chem. Phys.* **124**, 219906 (2006).
 - [42] G. Kresse and J. Furthmüller, *Phys. Rev. B* **54**, 11169 (1996).
 - [43] The standard value for the fraction of exact exchange of 0.25 and a plane-wave energy cutoff of 350 eV was used.
 - [44] M. J. Lucero, I. Aguilera, C. V. Diaconu, P. Palacios, P. Wahnón, and G. E. Scuseria, *Phys. Rev. B* **83**, 205128 (2011).
 - [45] Y. Zhang, X. Yuan, X. Sun, B.-C. Shih, P. Zhang, and W. Zhang, *Phys. Rev. B* **84**, 075127 (2011).
 - [46] S. Lany and A. Zunger, *Phys. Rev. B* **78**, 235104 (2008).
 - [47] G. Hanna, J. Mattheis, V. Laptev, Y. Yamamoto, U. Rau, and H. Schock, *Thin Solid Films* **431-432**, 31 (2003).
 - [48] T. Haalboom, T. Godecke, F. Ernst, M. Ruhle, R. Herberholz, H. W. Schock, C. Beilharz, and K. W. Benz, *Inst. Phys. Conf. Ser.* **152**, 249 (1998).
 - [49] C. Stephan, S. Schorr, M. Tovar, and H. W. Schock, *Appl. Phys. Lett.* **98**, 091906 (2011).
 - [50] J. T. Heath, J. D. Cohen, W. N. Shafarman, D. X. Liao, and A. A. Rockett, *Appl. Phys. Lett.* **80**, 4540 (2002).
 - [51] T. Eisenbarth, T. Unold, R. Caballero, C. A. Kaufmann, D. Abou-Ras, and H. W. Schock, *Thin Solid Films* **517**, 2244 (2009).
 - [52] M. Turcu, I. M. Kötschau, and U. Rau, *Appl. Phys. A* **73**, 769 (2001).
 - [53] J. Krustok, M. Collan, M. Yakushev, and K. Hjelt, *Physica Scripta* **T79**, 179 (1999).
 - [54] Since Koopman's theorem does not apply in density functional theory, the single-particle energies may differ from absorption and photoluminescence energies.